Journal of Applied Electrochemistry **34**: 771–780, 2004.

Measurement of polarization parameters impacting on electrodeposit morphology. II: conventional zinc electrowinning solutions

P.A. ADCOCK[1,†,*], A. QUILLINAN[2‡], B. CLARK[2§], O.M.G. NEWMAN[2] and S.B. ADELOJU[3,†]
[1]*MST-11, Los Alamos National Laboratory, PO Box 1663, MS D429, Los Alamos, New Mexico 87545, USA*
[2]*Pasminco Smelter Technical Support, PO Box 175, Boolaroo, New South Wales 2284, Australia*
[3]*School of Applied Sciences and Engineering, Monash University, Gippsland Campus, Northways Road, Churchill, Victoria 3842, Australia*
*(*author for correspondence, e-mail: palcadcock@hotmail.com)*
[†]*Formerly at Centre for Electrochemical Research and Analytical Technology, Building P (Penrith), University of Western Sydney, Locked Bag 1797, Penrith South DC, NSW 1797, Australia*
[‡]*Current address: Jacobs Engineering, Mahon Industrial Estate, Blackrock, Cork, Republic of Ireland*
[§]*Current address: Pasminco Port Pirie Smelter, PO Box 219, Port Pirie, South Australia 5540, Australia*

Received October 13 2003; accepted in revised form 19 March 2004

Key words: additives, electrodeposit morphology, nucleation, overpotential, zinc

Abstract

A new technique for measuring effects of polarization modifiers on nucleation potential and plating potential in polycrystalline electrodeposition was presented in Part I of this series (J. Appl. Electrochem. **32** (2002) 1101–1107). This paper presents the results of application of the proposed technique to conventional zinc electrowinning. Strong correlations are observed between deposit metallographic structure and the polarization characteristics. The results demonstrate that the new galvano-staircase method can be used to predict long-term (i.e. substrate-independent) deposit morphology, based on relatively rapid electrochemical measurements. With sufficient knowledge of the system, beneficial changes can be specified for additives, particularly long term averages. However even interactive, control on an hourly basis should be possible.

1. Introduction

The bulk of the world's zinc production, about 4 Mt annually, is produced by the electrolytic route [1]. This process, which uses cells with a large number of parallel plate electrodes, was first commercialized in 1917. A number of factors can impact on the current efficiency of zinc electrowinning. Nowadays, in the most mechanized operating plants, the current density, deposition time, and zinc and acid levels are all fixed, or vary little with time. Under these circumstances, deposit morphology and solution quality are the major considerations. In commercial zinc electrowinning cells, various morphology modifiers are widely used. To our knowledge only one operation, that of Asturiana de Zinc in Spain, claims [2] to use no such additives.

For zinc electrodeposition, correlations between deposit morphology and electrochemical polarization measurements have a long history. As far back as 1914, Pring and Tainton [3] reported on *in-situ* measurements of the plating potential for zinc deposition. In another work, Tainton [4] proved the importance of adequate cathode polarization for maximization of current efficiency. Many recent papers on zinc electrowinning have included some form of polarization measurements, mostly based on slow scan cyclic voltammetry [5]. In a few cases, other techniques were used [6–8].

Central to much existing literature on the morphological effects of polarization characteristics of conventional zinc electrowinning solutions are (i) the relationship illustrated by Andersen et al. [9] (reproduced in Figure 1) and (ii) the CEQM (continuous electrolyte quality monitor of 'nucleation potential') invented by Kerby et al. [10, 11]. In the Trail cellhouse of Teck Cominco, simple relationships were observed between 'nucleation overpotential' [11] and deposit morphology. It was even possible to use this parameter successfully as a one-dimensional surrogate for deposit morphology, and to control around an optimum point for current efficiency maximization. Based on this, several publications from various sources have also treated their own laboratory's version of Cominco's 'nucleation overpotential' (estimated from cyclic voltammetry curves), in isolation, as a surrogate parameter for deposit morphology. However, Figure 1 is a valid schematic for effects of *plating potential*. In the general situation, this is not correlated to effects on *nucleation potential*, by whatever method the latter parameter is

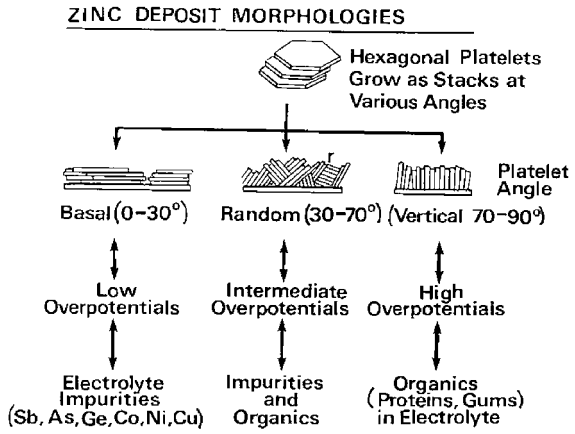

Fig. 1. Effects of zinc electrowinning additives according to the literature [10] (reproduced with permission from TMS).

measured, since it has been shown conclusively that various impurities affect different polarization parameters in diverse characteristic ways [12]. Adcock, Ault and Newman [13] drew attention to the fact that in other industrial situations, nucleation overpotential measurements alone may not necessarily correlate with morphology of the deposit. The optimum E_n value may move in an unpredictable manner in operations where parameters such as trace lead concentration [13], other impurities in solution [12], redox potential [14], another additive (e.g. mist suppressant) [13], electrolyte temperature, concentration of the plating metal (zinc) ion [13], or plating current density vary significantly.

In most cases, finding this optimum E_n value is a laborious process requiring the determination of a new set of current efficiency/E_n relationships by varying additive levels. In zinc electrowinning, surfactants are added for the purposes of acid mist suppression in many operations. However, published information on effects of additives other than antimony and glue or gelatin, including surfactants [13,15–17], is scarce. In situations such as these, it is very difficult to apply the original CEQM technique [10] or to use shifts in parameters from cyclic voltammograms to determine whether the additives are optimized.

This paper discusses a method with more general applicability for achieving a balance between the effects of smoothing agents and such parameters as those listed above. First we show a correlation between morphology and electrochemical polarization measurements for 28 different solutions containing various combinations of additives and impurities, but ignoring the specific species and levels present. The correlation method could be generalized with respect to current density. Only a significant change in temperature (by >10 K) or a change in the order of magnitude of concentration of the depositing ion might require a recalibration of the technique. In the context of this data, the experimentalist has an inbuilt ability to make predictions of how to alter the morphology towards a target (e.g. that which maximizes current efficiency, presumed to be the 'UD' type), without carrying out plating tests. This technique provides a more general, two-dimensional surrogate for deposit morphology. After that important section of the paper, some individual effects of additives, in the same system, on the critical polarization parameters are briefly surveyed. Certain interactions between additives are noted.

2. Experimental

2.1. *Details of polarization cell and electrodes*

The polarization cell (shown in plan view in Figure 2) consisted of a water-jacketed, glass beaker with inside dimensions of 56 mm diameter and 109 mm depth. An acrylic (plexiglass) lid of 80 mm diameter was milled on the lower surface, which was sealed with a viton o-ring. The lid was fitted over the filled beaker containing 200 ml of test solution. This lid contained slots for the support stems of two parallel electrode holders as well as a reference electrode and a thermometer/vent hole. The working and counter electrodes were interchangeable buttons made for a holder shown in Figure 3. The working electrode was a 12 mm diameter aluminum disc. The counter electrodes, of 11 mm diameter, were either of abraded zinc (Special High Grade; >99.9975%) used for the tests reported in Section 3.1, or else had an oxygen-evolving, mixed oxide-coated titanium (from Anode Technology, Ernest, QLD, Australia) piece attached by silver epoxy to a cylinder of fine, pore-free graphite, used for the tests reported in Section 3.2. Each complete cylinder was embedded in acrylic to produce an exchangeable button electrode. The buttons were held parallel with a separation of 2.0 cm. The coated titanium counter electrode usually only required rinsing and an ultrasonic clean with Milli-Q® water in between scans. Whenever a zinc counter electrode was used, it was abraded to a P600 finish, rinsed, and cleaned ultrasonically. The reference electrode was a Ag|AgCl:KCl (3 N) electrode fitted with a

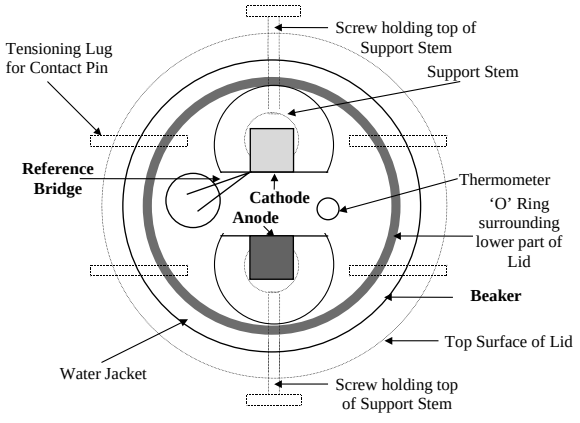

Fig. 2. Plan view of cell for polarization measurements.

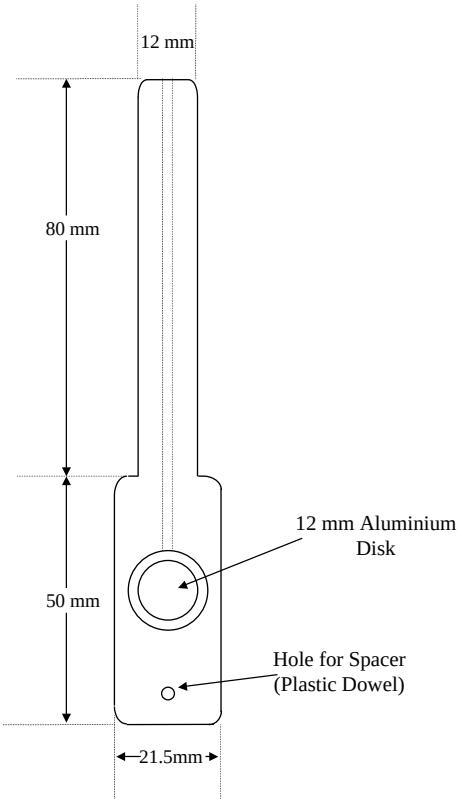

Fig. 3. Button electrode holder (for the cathode).

KCl-filled bridge tube and Vycor tip. All data are reported after offline IR-compensation, but no liquid junction potential correction has been applied.

2.2. *The working electrode and its surface preparation*

The substrate investigated in the present work was air-oxidized 4 nines (99.99%) aluminum, which, according to the supplier, contained Mg, Si, Cr, Fe, Cu, and Ga at 0.001% and B, Na, Ti, V, Mn, Ni, Zn, Sn, and Pb below 0.001%. Cyclic voltammetry experiments on zinc electrolytes have been shown to be highly sensitive to the purity and composition of the aluminum working electrode [18, 19]. The safest path for polarization studies on zinc electrowinning appears to be to use only high purity aluminum, air oxidized between polishing and use. As pointed out previously [20], after each use, the working electrodes must be polished to remove traces of zinc, but a polished aluminum electrode cements solution impurities, (e.g. copper) and gives an anomalous scan, if there is insufficient time for the protective alumina layer to be restored. A 36-h delay between polishing and use produced stable behaviour and excellent reproducibility.

It was imperative that, after every use, each working electrode was removed from its holder and soaked in a 'pickle solution' (a 4 N mixture of sulfuric acid and some zinc sulfate), at ≥35 °C for at least 10 min (until bubbles no longer appeared on the surface). To remove all sulfate, the electrode was then rinsed, cleaned ultrasonically for 2 min, and rinsed again, using Milli-Q® water for each rinsing step. For new working electrodes, coarse wet grinding with silicon carbide papers was taken through to the P600 stage with abrasion in the vertical direction. For these or for used and pickled electrodes, fine grinding stages with P1200 to P4000 papers, in the vertical direction were applied. Inter-stage cleaning was carried out in Milli-Q® water in an ultrasonic bath for 2 minutes. After finally rinsing with Milli-Q® water, all electrodes were dried with exposure to air for at least 36 h.

2.3. *Addition agents*

All stock and dosing solutions were made using Milli-Q® grade water. AR grade $K(SbO)(CO_2\ CHOH\ CHOH\ CO_2).{}^1/_2\,H_2O$ was dissolved at 700 mg l^{-1} and dosing solutions were made by further dilution of this stock solution. AR grade $Pb(CH_3COO)_2.3H_2O$ was used to prepare a solution containing 1 g Pb l^{-1} for dosing.

Glue was Davis 'EZ grade' animal glue. Fine Gelatin powder was supplied by Rousselot (Belgium). For each of these reagents, a 10 g l^{-1} stock solution containing 1 g NaOH l^{-1} was used. Licorice ('SAIL grade' spray dried extract from CMC Australia Pty Ltd) was dissolved at 10 g l^{-1} in pre-mixed NaOH solution (1.67 g l^{-1}).

Tutogen Mk IV was supplied as a concentrated solution by Industrial Products Marketing. A 20 g l^{-1} dilution of this material was used as stock solution. Bevaloid 6794 commercial concentrated solution was acquired from Pasminco's Budel operation (Netherlands). A 5 g l^{-1} dilution of this material was used as stock solution.

In the continuous process for conventional zinc electrowinning, neutral feed solution blends in a ratio of about 1:20 with recycled spent electrolyte, which is highly acidic (>150 g $H_2SO_4\,l^{-1}$) and contains about a third of the concentration of zinc sulfate found in the neutral feed. Spent electrolyte is therefore more representative of the process solution than is neutral feed itself. In this study, electrolytes, termed 'simulated spent', were prepared by dilution and acidification of neutral feed solution. Mn(III), normally found in spent electrolyte, but not in neutral feed, was produced by addition, with vigorous agitation, of a known amount of $KMnO_4$, which reacted quantitatively with Mn(II) already present in the solution in excess.

2.4. *Experimental method*

The galvano-staircase technique used in this study consisted of three segments, as described in Figure 4 and Table 1 of the earlier paper [20]. The first segment, designed to find the nucleation potential, was taken at a very slow scan rate. This was followed by a rapid scan to the maximum current density (80 mA cm^{-2}, i.e. above the normal industrial current density), and then a reverse scan at a moderate scan rate. Each scan consisted of a series of steps at half-second intervals,

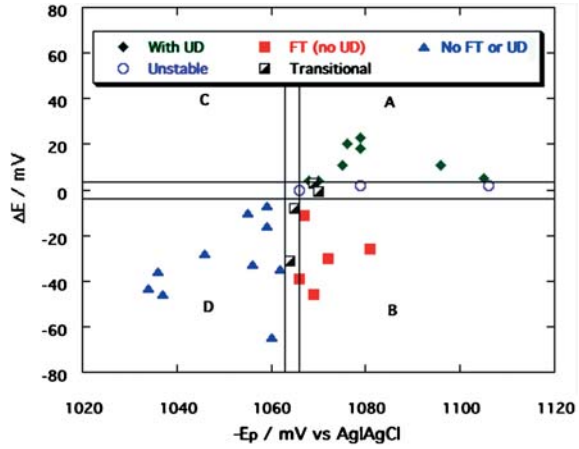

Fig. 4. Morphological type for 3-h deposit plotted according to polarization characteristics measured using zinc (>99.9975%) counter electrode.

designed to give a stable potential reading, essentially free of charging current effects. The nucleation potential, E_n, was taken as the reading for the step immediately after the most cathodic potential reached. The plating potential was taken at 60 mA cm^{-2} on the reverse scan. The data were taken with a Princeton Applied Research 263 or Versastat II instrument, controlled through a National Instruments PCII/IIA GPIB card by routines written for DOS-based software, which was run in a Windows 3.11 shell. The results were exported to spreadsheets, for IR-correction and analysis. For the IR-correction, the appropriate value of uncompensated resistance was determined using a square-wave procedure described elsewhere [21]. The measurement of nucleation and plating potentials by the galvano-staircase technique is very reproducible, with a standard deviation of 3 mV or less.

2.5. *Formation and examination of electrodeposits*

Electrowinning tests were based on a system similar to the 'mini-cell' setup described by Gonzalez-Dominguez and Lew [22]. The button electrodes and holder were like those used for polarization measurements, but the aluminum was of the alloy grade used for cathodes in Pasminco's industrial cells. The counter electrode was of 99.9975% zinc. The cell had sufficient volume (1 l) to ensure that deposition for 3 h had negligible effect on the bulk solution composition. A set of 3-h deposits was obtained and used for this investigation. After stripping, the 3-h deposits were mounted in an epoxy resin and cross-sectioned then ground flat and polished to a 1 μm diamond finish before finishing with Struers OP-S suspension on OP-Chem cloth. The polished deposits were etched, by dipping for two seconds or less in an aqueous solution of CrO_3 (200 g l^{-1}) and Na_2SO_4 (15 g l^{-1}), and brightened by a 5 s dip in aqueous CrO_3 (200 g l^{-1}), degreasing, rinsing and drying according to recommendations in the literature [23]. The deposits thus prepared were examined under a stereo microscope, with photographs being obtained for determination of the metallurgical types [24–26].

3. Results and discussion

3.1. *Correlation between polarization characteristics and metallographic structure*

In order to prove the utility of the new galvano-staircase technique, complementary studies in deposition cells were coupled to galvano-staircase measurements. The polarization characteristics were measured, on portions of fresh simulated spent electrolytes with 50 mg $KMnO_4$ l^{-1} added, as prepared for 3-h electrodeposition tests. Electrolytes of varying purity and containing different levels of a wide variety of additives and their combinations were tested. As will be seen below, it would be appropriate also to study in the same way, the electrochemical characteristics of used solutions taken from continuous, or short-term batch electrodeposition experiments.

Table 1. Typical IR-Corrected Data for Freshly Added Dopants to Fresh, Simulated Hobart Electrolyte at 38 °C

Dopants /mg l^{-1}	$-E_n$ /mV vs Hg/Hg_2SO_4	$-E_p$ /mV vs $Hg/HgSO_4$	ΔE /mV	Zone
None	1168	1067	−101	B
Sb (0.01)	1122	1054	−68	D
Sb (0.02)	1120	1059	−61	D
Pb (0.5)	1117	1069	−48	B
Pb (3.0)	1179	1089	−90	B
Glue (5)	1136	1104	−32	B
Glue (15)	1188	1117	−71	B
Licorice (10)	1137	1106	−31	B
Licorice (15)	1119	1112	−7	B[a]
Licorice (20)	1169	1109	−60	B
Tutogen MkIV (10)	1135	1100	−35	B
Tutogen MkIV (30)	1149	1103	−46	B
Gelatin (15)	1151	1110	−41	B
Bevaloid 6794 (7.5)	1147	1085	−62	B

[a] With correction for polishing technique, this is in the B to A transitional zone.

In the theoretical considerations presented previously [20], ΔE was defined as $E_n - E_p$, where E_n is the observed nucleation potential and E_p is plating potential at the current density of interest. Frequent tri-dimensional nucleation during deposit growth requires little or no remaining energy barrier. Therefore E_n should not be much more cathodic than E_p. If the substrate behaves ideally, this will translate to a need for a positive value of ΔE. In general, grain size should decrease as ΔE increases, because there will be more secondary nucleation events. On the other hand, 'leveling' was anticipated previously to require at least some critical value of plating overpotential [20]. To summarize the theory [20], moving to more negative E_p is expected to produce leveling, and moving towards a positive ΔE is expected to produce grain refinement.

Figure 4 shows the data plotted according to the pattern outlined previously (in Figure 3 of [20]). For discussion purposes, Zones A to D are defined quantitatively as follows for zinc deposition at 38 °C from a solution of composition (50 g Zn l^{-1} with excess H_2SO_4) typically used for zinc electrowinning. Zones A and C are defined for $\Delta E \geq +4$ mV, and Zones B and D for $\Delta E < -4$ mV. Zones A and B are defined for $-E_p \geq 1066$ mV vs Ag|AgCl and Zones C and D for $-E_p < 1063$ mV vs Ag|AgCl. This procedure is similar to a technique of analysis used previously by Kerby [27]. Five narrow zones in two intersecting bands exist between these four major zones. In contrast, Kerby's schematics [27] envisaged nine zones, all of roughly equivalent size.

In Figure 4, the finest grained deposits were mostly found towards the top of the diagram, as expected. However, levelness did not correlate directly with moving towards the right of Figure 4. 'Leveling' is a complex morphological phenomenon, dependent on many factors. In Figure 4, there may be an optimum range near the centre of the diagram. The two most level deposits had $-E_p$ values of 1067 and 1079 mV. However, some deposits with values in between the two mentioned were pinholed. The phenomenon of pinholing is not specifically dealt with by the Winand theory [25]. It can be anticipated to be a function of interfacial tensions between gas, liquid, and solid phases. These in turn are very sensitive to the presence or absence of surfactants, the behavior of which can depend markedly on concentration relative to critical micelle concentration. An example of the complex effects of a surfactant (licorice) is discussed in Section 3.2, below.

In Figure 4, there are no points in Zone C. This zone corresponds to a low plating overpotential and a positive ΔE. The characteristics for fine, powdery FI (field-oriented, isolated) deposits shown on the Winand diagram [25] suggest that Zone C characteristics could occur when there is a combination of concentration polarization (e.g. low zinc concentration) and a lack of strong inhibitors.

There are ten entries, all shown with triangles, for Zone D, which corresponds to a low plating overpotential and a negative ΔE. Our theory [20] predicts that deposits formed under these conditions will be BR (basis reproduction) and/or non-powdery FI types. Those to the far left of the diagram (Figure 4) tend to be rough BR deposits with FI type islands mixed in, the poorest quality deposits, e.g. Figure 5(a). As the vertical band before Zone B is approached, level, BR structured deposits of improved quality are obtained, e.g. Figure 5(b). Solutions corresponding to Zone D conditions generally contained low levels of organic inhibitors and/or high Sb.

Five data points, all shown with filled squares in Figure 4, occurred inside Zone B, which corresponds to a high plating overpotential, but a negative ΔE. The theory [20] predicts that the growth mode should be FT (field-oriented, textured) type. FT type growth did appear in this zone, but the deposits were mostly of mixed FT and BR type, an example of which is shown in Figure 5(c). In the narrow transition zone between Zone D and Zone B, the two deposits showed unusual features. One had uncharacteristically fine grain size for its vertical position and the other was severely pinholed.

Eight data points, all shown with diamonds in Figure 4, fell in Zone A, the conditions for which are a significantly positive ΔE and a high plating overpotential. The theory predicts this zone as the most likely to produce UD deposits, which are expected to be smooth, fine-grained, and the optimal morphology for zinc electrowinning. In Zone A, finer-grained deposits are obtained, as shown in Figure 5(d). At high magnification, however, all of these deposits appeared to have some texture, though not necessarily resembling the FT texture of Figure 5(c), which remains to some extent in the deposit shown in Figure 5(d). These experiments had gelatin or another polarizing organic additive present.

Careful examination of the deposit morphology from Figure 5(a)–(c) shows that the grain orientation altered, with little change in grain size. However, the examination of deposit morphology from Figure 5(c)–(d) reveals that the major change is a reduction in grain size. Hence, the vertical direction in Figure 4 relates to grain size (and microroughness) and the horizontal direction to grain orientation, which affects the macroroughness. This is consistent with the theoretical considerations given earlier [20]. The morphology of Figure 5(d), corresponding to Zone A, is an optimal one. However, high current efficiency, and good deposit stripping characteristics can also be obtained for deposits in other zones but close to the transition to Zone A.

In the transition zone below zone A, various morphologies were observed. Two (indicated with half-filled squares in Figure 4) showed different degrees of pinholing, grain refinement, and transition from a basis orientation (BR) to a field orientation (FT), and therefore are classed as transitional. Another three deposits showed a mixture of UD (or pseudo-UD [28]) and FI, producing a very wavy surface. We interpret this as a particular morphological instability, as indicated in

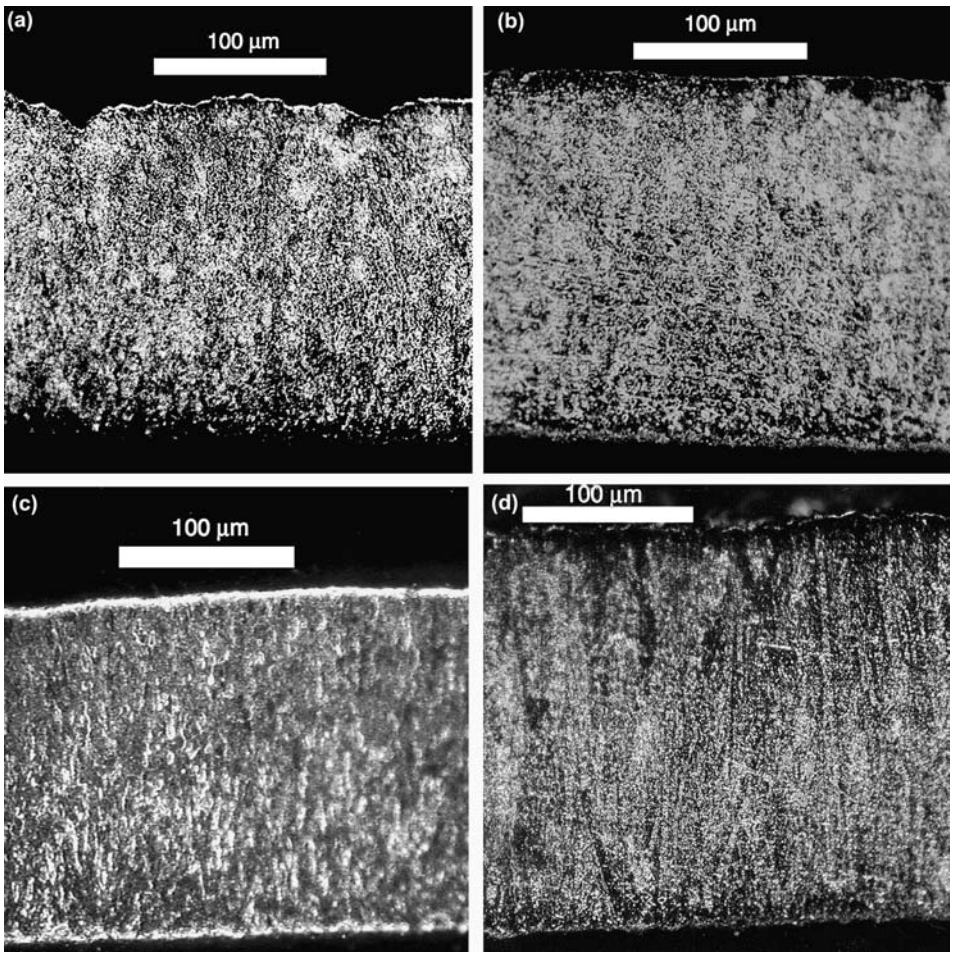

Fig. 5. Photomicrographs of typical deposits from (a) left hand area of Zone D, (b) right hand area of Zone D, (c) Zone B, (d) Zone A. Note: (d) was photographed towards rim of deposit; others near centre.

Figure 4, using circles. The current efficiency for the latter three deposits was much reduced, which would put them in a different hydrodynamic regime from the others – modified by the effects of vigorous hydrogen evolution [29]. Because of this change in hydrodynamics, a different slice through the Winand diagram, at a lower J/J_d may be relevant to these deposits and/or the corresponding galvano-staircase scans.

According to Winand [25], the overlap between deposits of different types is very wide. However, the correlation between cross sectional structure and polarization characteristics in Figure 4 is strong, and overlaps are confined to small regions. However, there would be a smearing of these demarcations, if a parameter, such as temperature, zinc concentration, or diffusion layer thickness were altered by a large amount, and this may explain in part, the pessimistic view of Winand.

3.2. *Polarization effects of individual species*

The galvano-staircase method was used to compare polarization effects of a number of electrowinning additives in a synthetic solution designed to simulate conditions in Pasminco's Hobart cells (i.e. a simulated spent). The blank solution was prepared from neutral, pure solution by dilution, acidification and addition of $KMnO_4$ (80 mg l^{-1}). Some organic inhibitors were tested at a number of different concentrations. In the previous section, polishing of working electrodes was taken through to P4000, but in the remainder of this paper, it was stopped at P2400. Based on results presented previously [20], the effect of this change is expected to be about $+3$ mV on $-E_n$, nil on E_p, and -3 mV on ΔE. Table 1 and Figure 6 present typical data for a range of cell additives used in various Pasminco cellhouses. These data were also obtained at 38 °C with the plating potential being measured at 600 A m^{-2}.

The data in Table 1 are single measurements on fresh electrolytes. Figure 6 includes some data for which additional additive was added to a batch of electrolyte previously used for at least one galvano-staircase scan. Such a 'used' solution will have been electrolysed with the same polarity as in an electrowinning cell, but over a wide range of current densities. Hence, reagent modification involving certain electrochemical reactions is possible, as discussed further on for the specific case of antimony. In fresh solutions, the nucleation potential responded to changes in glue level, whereas in used solutions, the nucleation potential was insensitive to changes in glue above a threshold effect. However, in

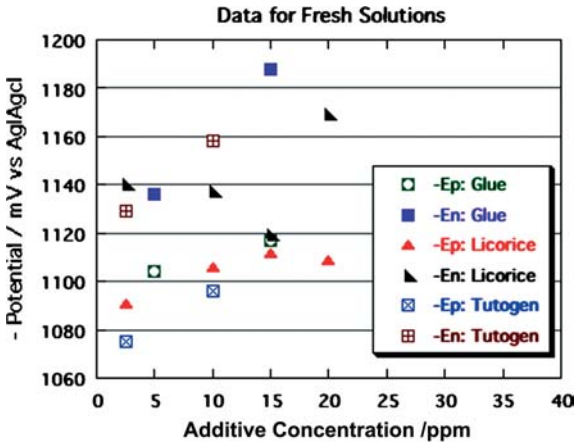

Fig. 6. Polarization data for gelatin, licorice and Tutogen in fresh electrolytes, measured using mixed oxide coated titanium counter electrode.

used solutions, the nucleation potential showed enhanced sensitivity to antimony, as will be discussed in the following section.

Taking $-E_p$ as the indicator of inhibition intensity, we can define the polarizing power of the specific additive as the increase in $-E_p$ compared to addition-free electrolyte. Licorice was studied in the most detail. With this additive, the polarizing power is initially proportional to the square root of the concentration, but later a plateau is reached. For comparable addition rates on a weight/volume basis, polarizing power decreases in the order:
animal glue > gelatin ~ licorice > Tutogen Mk IV > Bevaloid 6794.

The behaviour of $-E_n$ is more complex. A low concentration of any of the substances tested lowered the overall energy barrier to nucleation (i.e. made E_n less cathodic). With the exception of antimony, most substances tested over a range of concentrations (including lead, glue, licorice and Tutogen Mk IV) increased the nucleation overpotential again with increased concentration. The effect of low concentrations of organic substances is believed to relate to a change in surface tension, which is independent of the overall polarizing effect of these additives, seen in the effect on the plating potential. There are precedents in the literature for an initial fall in 'nucleation overpotential' (measured by cyclic voltammetry) followed by an increase for organic inhibitors including glue [15] and saponin [17]. Minima in the 'nucleation overpotential' vs concentration curves have also been reported for licorice, Dowfroth 250, Yucca, and *m,p*-cresol [17]. To our knowledge, these effects have never been fully explained. However, if the nucleation overpotential, $-\eta_n=-(E_n-E_{Rev})$ [30] is considered as a function of surface tension (or its microscopic analogue, surface energy) raised to the power 3/2 [25, 31], it would be predicted that surfactant molecules would induce a major initial drop in value [32]. What happens at higher surfactant concentration would depend on the tendency to form micellar aggregates, surface monolayers, and so forth [32].

Figure 1, taken from previously existing literature, is simpler than Figure 4 or the Winand diagram. In Figure 1, the randomly-oriented (or unoriented, 'UD') type occurs in between the basal 'BR' and vertical 'FT' types, in apparent disagreement with the Winand Diagram [33]. However, it will be seen below how both views can be reconciled. Returning to the above quantitative definitions of Zones A to D for a temperature of 38 °C, the blank solution had co-ordinates at the lower left of Zone B. Lead additions confirmed Zone B characteristics. However, adding antimony altered the characteristics to Zone D by reducing plating overpotential. This agrees with a shift to the far left in Figure 1. Surfactants produced Zone B characteristics, but in some cases, such as with 15 ppm Licorice, there was an approach towards Zone A. In Figure 6, the effect of licorice on plating potential reaches a plateau at a concentration of about 15 mg/l, at which point the nucleation overpotential is near a minimum. Adding more licorice results mainly in a sharp increase in nucleation overpotential. Thus the polarization characteristics move from near Zone A back to the centre of Zone B. One could imagine conditions for switching from Zone B to Zone A, and back again, as the reagent concentration increases. Organic inhibitors produced Zone B characteristics. It is known that deposits of strong FT type, which are brittle and usually difficult to strip, can be formed with an excess of a polarizing agent. These deposits should fall into Zone B. The effect of excess inhibitor or surfactant is comparable to that described by Figure 1, a shift to the right. The present work suggests that sometimes the desirable morphology, shown in the center of Figure 1, can be elusive, if the additives used are incapable of producing the correct combination of nucleation and plating potentials. In addition, the differences between Figure 1 and the Winand diagram can be understood.

3.3. *Special note on the behavior of antimony*

It was seen in Table 1 that nucleation potential is very sensitive to antimony, and that the effects are neither linear, nor monotonic. In zinc electrowinning, it is well known that a small addition of antimony (perhaps 40 ppb) can be beneficial, but that 100 ppb or more is detrimental. It is also known that there are different effects depending on whether Sb exists in the +3 or the +5 oxidation state [14]. Figure 7 shows that the magnitude of the effect of antimony differs in fresh and used solutions, due to electrolysis and ageing effects. The differences are probably due to changes in the distribution of the various forms of antimony present in the solution. These effects of Sb appear to be more complex than those already explained in the literature [14]. Using simulated Hobart spent electrolyte, containing a significant level of Mn(III), fresh electrolytes displayed a nucleation gap, *E*, approaching a zero or positive value only for limited concentration ranges and mixtures of additives. Simulation of a spent electrolyte is

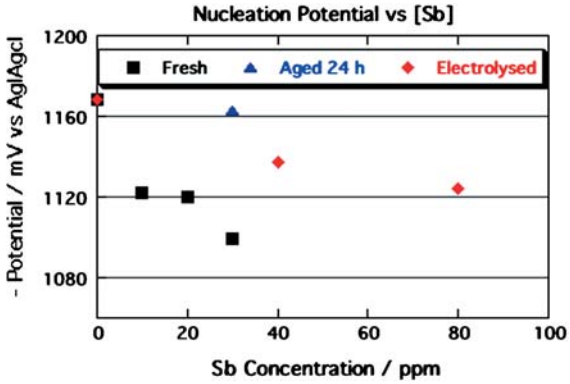

Fig. 7. Sensitivity of the effect of antimony on nucleation potential to electrolysis or ageing of the solution, measured using mixed oxide coated titanium counter electrode.

difficult when antimony is involved. It is hypothesized that the difference between fresh and used solutions should disappear if an electrolyte contains zero antimony or similar elements. This was true for additive-free solution in Figure 7.

The results in Figure were all obtained using mixed oxide coated titanium counter electrode. It is possible that zinc or oxidized lead (or lead alloy) anodes could produce different results. Recently-sampled spent electrolytes typically analyse at a significantly lower Sb concentration than the total Sb concentration fed to the system. For these reasons, for precise calibration of a given industrial operation, a correlation (as in Figure 4, which was obtained on duplicate portions of fresh simulated spent electrolytes prior to electrolysis) should be obtained by comparing galvano-staircase measurements on electrolysed spent solutions with the morphology of deposits already obtained from the very same solutions.

3.4. *Industrial application to additive optimization*

Recently, at Pasminco Hobart Smelter, there was difficulty obtaining ductile deposits and high current efficiencies at or above 38 °C. The additives in use were licorice, Tutogen Mk IV and antimony (as KSbO.tartrate). A partial factorial study using the galvano-staircase technique on fresh electrolytes containing Mn(III) was carried out. Generally very negative values of ΔE were obtained (less so on used electrolytes). This was considered to be an indication of too high an addition rate of Sb, which was confirmed by subsequent small-scale electrolysis tests. Hence, a reduction in Sb additions to the plant cell units was recommended, tested, and finally adopted at the Hobart site. Likewise, an increase in the ratio of licorice to Tutogen was recommended, tested further, and eventually adopted at the site. These two changes, guided by measurements plotted according to the axes of Figure 4, allowed efficient operation at higher temperatures than before. Knowledge gained concerning the licorice/Tutogen interaction might be even more useful if additions of all three reagents could be controlled independently – Tutogen being used as the principal acid mist suppressant, and licorice and antimony being varied to control the morphology.

3.5. *Future prospects for the galvano-staircase technique*

Based on the data reported here, galvano-staircase measurements of the nucleation potential and of metal plating polarization curves seem to offer significant advantages over cyclic voltammetry and all other previous approaches to the control of morphology based on cathode polarization measurements. These measurements give an improved characterization of the effects of individual additives, and of the net effect of all additives and residual impurities in an electrolyte, as examined and discussed in Sections 3.2–3.4. In Section 3.1, the position on a diagram such as Figure 4 was found to correlate strongly with deposit metallurgical structure, under conditions of a steady, high metal ion concentration, steady hydrodynamic conditions, and constant temperature. The technique represents a surrogate for laborious characterization of morphology at every step of modification of additives to achieve the preferred type of growth. Pasminco has used this technique to optimize the levels of smoothing agent, surfactant and antimony in the cell additive mixture, as described in Section 3.4.

For studies of zinc nucleation and growth kinetics, we do not claim that surface-oxidized aluminum is the ultimate substrate, even though its behaviour approaches ideality. To understand nucleation potentials better, research is needed on other substrates, such as glassy carbon or highly oriented pyrolytic graphite (HOPG). Further studies coupled to electrodeposition tests and comparison of results with those of other techniques are warranted for various metal electrodeposition systems, altering the anion, and most importantly, the depositing metal ion. If the results are positive, it may become possible to formulate general guidelines for using the galvano-staircase technique to screen a wide range of new conditions in a short time. At

this point, such parallel studies of polarization characteristics and deposit morphologies have been carried out on zinc electrodeposition from electrolytes containing a high level of iron. These studies will be reported in a future publication.

Utilization of the knowledge of the type of relationship, seen in Figure 4, could increase productivity in the areas of basic applied research, as well as plant practice. We believe the applicability of the method should be extendable to other processes involving electrocrystallization of a polycrystalline metal deposit, in which the influence of the solution characteristics predominates over that of the substrate [34, 35]. We foresee potential, specific applications of the galvano-staircase technique in:

(a) everyday process monitoring, troubleshooting, and control;
(b) streamlining R&D on new processes, especially selection of appropriate additives;
(c) quality control on supply of additives;
(d) studies of the lifetime of stock additives; and possibly
(e) studies of additive modification/degradation in the electrolyte.

In addition, extension to studies of substrate-dependent morphology in thin films may be possible, by studying the competition between nucleation and grain growth on the actual deposition substrate.

4. Conclusions

1. The method proposed earlier for using polarization measurements to predict the cross sectional structure of metal electrodeposits has been demonstrated for the specific case of conventional zinc electrowinning. The morphological type was affected in different ways by plating overpotential and the gap between nucleation potential and plating potential, in a manner consistent with the theory presented earlier in Part I. For a given temperature and plating current density, when the gap between the two potentials specified was plotted against plating potential, four major zones (three being populated) were identifiable, which correlated strongly with cross sectional morphology. There were narrow, transitional bands between the main zones.
2. For a given solution, the zone in which these characteristics was located, was a strong but complex function of the concentrations of organic inhibitors, strongly depolarizing impurities such as antimony, and oxidant species. Over limited concentration ranges, several organic additives, including gelatin, actually reduced the nucleation overpotential, leading to some grain refinement.
3. For existing industrial operations, the new technique can provide a comprehensive picture of complex interactions between the polarization effects of various additives and impurities. It provides a two-dimensional surrogate for deposit morphology with an inbuilt ability to assist process operators to optimize additive mixtures and cathode deposit quality, and to maximize current efficiency.
4. The method also appears extremely useful as part of any medium- to large-scale research program into new electrolyte systems or conditions for electrowinning zinc. The principles should also be applicable to many other metals and electrodeposition processes for thick deposits. By using a real substrate for deposition as the substrate for galvano-staircase measurements, electrochemical parameters for prediction of morphologies of electrodeposited thin films may also be possible.

Acknowledgements

PA is grateful to UWS for the provision of an Australian Postgraduate Award and to Pasminco Limited for a Top-up Scholarship. The authors also thank Dr. C.S. Lakshmi (Pasminco) for sample mounting, Mr. Geoff Hansen (CSIRO) for development of the polishing technique, Mr. Tom Bradley (Macquarie University) for the sample polishing, Mr. Curt Stocksiek (UWS) and Dr. Fernando Garzon (LANL) for the use of microscopes and photographic equipment, Mr. Noel Bradford for assistance with preparation of the drawings, and finally Pasminco Limited for permission to publish this paper.

Appendix A.: List of Symbols and Acronyms

BR	basis-reproduction type
CEQM	continuous electrolyte quality monitor
ΔE	$E_n - E_p$, 'nucleation gap'
E_n	nucleation potential
E_p	plating potential
E_{Rev}	reversible potential
FI	field-oriented, isolated crystals type
FT	field-oriented, texture type
$-\eta_n$	$E_{Rev} - E_n = -(E_n - E_{Rev})$, nucleation overpotential
UD	unoriented dispersion type

References

1. J.W. Evans, *Met. Mat. Trans. B* **26** (1995) 189–208.
2. F.J. Tamargo and Y. Lefevre, *in* T. Azakami, N. Masuko, J.E. Dutrizac and E. Ozberk (Eds), 'Zinc & Lead '95', (MMIJ, Tokyo, 1995), pp. 697–706.
3. J.N. Pring and U.C. Tainton, *J. Chem. Soc.* **105** (1914) 710–724.
4. U.C. Tainton, *Trans. Am. Electrochem. Soc.* **41** (1922) 389–410.
5. B.A. Lamping and T.J. O'Keefe, *Met. Trans. B.* **7** (1976) 551–558.
6. S. Ohyama and S. Morioka, *in* K. Tozawa, (Ed), 'Zinc 85: Proceedings of the International Symposium on Extractive Metallurgy of Zinc', (MMIJ, Tokyo, 1985), pp. 219–234.
7. M. Maja, N. Penazzi, R. Fratesi and G. Roventi, *J. Electrochem. Soc.* **129** (1982) 2695–2700.
8. F. Noguchi, T. Nakamura and M. Sakata, *in* T. Azakami, N. Masuko, J.E. Dutrizac and E. Ozberk (Eds), 'Zinc & Lead '95', (MMIJ, Tokyo, 1995), pp. 404–413.
9. T.N. Andersen, R.C. Kerby and T.J. O'Keefe, *J. Metals* **37**(1) (January 1985) 36–43.

10. R.C. Kerby, H.E. Jackson, T.J. O'Keefe and Y.-M. Wang, *Met. Trans. B* **8** (1997) 661–668.
11. R. Kerby and C. Krauss, *in* J.M. Cigan, T.S. Mackey and T.J. 'O'Keefe (Eds), 'Lead-Zinc-Tin '80', (TMS–AIME, Warrendale, 1980), pp. 187–203.
12. D.J. Mackinnon, J.M. Brannen and P.L. Fenn, *J. Appl. Electrochem.* **17** (1987) 1129–1143.
13. P.A. Adcock, A.R. Ault and O.M.G. Newman, *J. Appl. Electrochem.* **15** (1985) 865–878.
14. R. Singh, T.J. O'Keefe, R.C. Kerby and K. Jibiki, *in* K. Tozawa, (Ed), Zinc '85: Proceedings of the International Symposium on Extractive Metallurgy of Zinc'; (MMIJ, Tokyo, 1985), pp. 235–250.
15. D.J. Mackinnon, R.M. Morrison, J.E. Mouland and P.E. Warren, *J. Appl. Electrochem.* **20** (1990) 728–736.
16. I.H. Warren, K. Tozawa, (Ed), 'Zinc '85: Proceedings of the International Symposium on Extractive Metallurgy of Zinc', (MMIJ, Tokyo, 1985), pp. 251–264.
17. A.M. Alfantazi, D.B. Dreisinger, M. Boissoneault and J. Synnot, *in* D.B. Dreisinger, (Ed), 'Aqueous Electrotechnologies: Progress in Theory and Practice', (TMS, Warrendale, 1997), pp. 139–161.
18. M.J. Howell, 'Techniques for monitoring the quality of industrial zinc suphate electrolytes', Honours Thesis, (University of Tasmania, 1991).
19. M.J. Howell, A.R. Ault, O.M.G. Newman, K.J. Cavell and B.V. O'Grady, *in* I.G. Matthew (Ed), 'World Zinc '93' (AusIMM, Melbourne, 1993), pp. 307–314.
20. P.A. Adcock, S.B. Adeloju and O.M.G. Newman, *J. Appl. Electrochem.* **32** (2002) 1101–1107.
21. P.A. Adcock, 'Zinc Electrowinning in the Presence of Iron(II)', Ph.D. Thesis, (University of Western Sydney – Nepean, 1999), pp. 190–213.
22. J.A. Gonzalez-Dominguez and R.W. Lew, *J. Metals* **37**(1) (1995) 34–37.
23. L. Mongeon and R.J. Barnhurst, Revision Authors, *in* 'Metals Handbook', Vol. 9, 9th ed., (ASM, Metals Park, 1985), pp. 488–496.
24. H. Fischer and H.F. Heiling, *Trans. Inst. Metal Finishing* **31** (1954) 90–102.
25. R. Winand, *Hydrometallurgy* **29** (1992) 567–598.
26. E. Budevski, G. Staikov and W.J. Lorenz, 'Electrochemical Phase Formation and Growth', (VCH, Weinheim, 1996), pp. 263–265.
27. R.C. Kerby, *US Patent 4 443 301* (1984).
28. R. Winand, *J. Appl. Electrochem.* **21** (1991) 377–385.
29. L. Vanhée, J.C. Monnier, R. Winand, and M. Stanislas, *J. Appl. Electrochem.* **24** (1994) 303–309.
30. H. Fischer, *Angew. Chem. Int. Ed. in Engl.* **8** (1969) 108–119.
31. E. Budevski, G. Staikov and W.J. Lorenz, *op. cit.* [26], p. 163.
32. A.W. Adamson, 'Physical Chemistry of Surfaces', 5th ed., (Wiley-Interscience, New York, 1990), pp. 508–513.
33. P.A. Adcock, S.B. Adeloju and O.M.G. Newman, *in* J.A. Gonzalez, J.E. Dutrizac, and G.H. Kelsall (Eds), 'Electrometallurgy 2001', (CIM, Montreal, 2001), pp. 401–414.
34. R. Winand, *Electrochim. Acta* **39** (1994) 1091–1105.
35. R. Winand, *in* I.H. Warren (Ed), 'Application of Polarization Measurements in the Control of Metal Deposition', (Elsevier, Amsterdam, 1984), pp. 47–83.